

## MULTI-DIRECTIONAL STRUCTURAL COMPONENT HYBRID TESTING SYSTEM FOR THE ASSESSMENT OF THE SEISMIC RESPONSE OF STEEL I-SHAPED COLUMNS

**Karl Auger\*, Yasaman Balazadeh-Minouei\*, Ahmed Elkady\*\*, Ali Imanpour\*\*, Martin  
Leclerc\*, Dimitrios Lignos\*\*\*, Guillaume Toutant\*, and Robert Tremblay\***

\* Department of Civil, Geological & Mining Engineering, Polytechnique Montreal, Canada  
e-mails: karl.auger90@gmail.com, yasaman.balazadeh-minouei@polymtl.ca, martin.leclerc@polymtl.ca,  
guillaume.toutant@polymtl.ca, robert.tremblay@polymtl.ca

\*\* Department of Civil Engineering & Applied Mechanics, McGill University, Montreal, Canada  
e-mails: ahmed.elkady@mail.mcgill.ca, ali.imanpour@mail.mcgill.ca

\*\*\* School of Architecture, Civil & Environmental Engineering, Swiss Federal Institute of Technology,  
Lausanne (EPFL), Switzerland, e-mail: dimitrios.lignos@epfl.ch

**Keywords:** Structural testing system, Seismic load, Cyclic test, Hybrid test, Steel I-shaped columns.

**Abstract.** *The Multi-Directional Hybrid Testing System (MDHTS) at Polytechnique Montreal is an advanced structural testing system that can be used to study the response of large-scale structural components such as columns, walls, or bridge piers subjected to any combination of displacements and forces along 6 degrees of freedom in static, quasi-static cyclic, pseudo-dynamic, or hybrid tests. This paper describes the main features, components and capacity of the MDHTS used for the seismic testing of steel I-shaped columns. Results of 3D finite element analysis performed to develop the test program and validate the test setup are presented. Three examples of tests on steel columns for concentrically braced frames (CBFs) and moment-resisting frames under seismic and multi-directional cyclic loadings are described. Furthermore, the hybrid simulation system is described and challenges faced when testing specimen exhibiting limited capacity are discussed. The MDHTS is an effective experimental tool to generate reliable data on steel column limit states under inelastic cyclic demands including any combination of local and global geometric instabilities with fixed and flexible boundary conditions.*

### 1 INTRODUCTION

Large-scale physical testing is a robust method to assess the seismic behaviour of structural components of buildings or bridges under earthquake loading. Experimental studies also aim at validating numerical simulations that are used to evaluate the inelastic response of seismic force-resisting systems. Quasi-static testing of structural components is a common structural testing method in earthquake engineering. In this method, the seismic induced loading is applied statically and dynamic effects are not taken into account. Earthquake demands, in the form of forces and displacements, are applied to test specimens using single or multiple actuators. The use of multiple actuators offers an opportunity to investigate the behaviour of structural components under a combination of forces and displacements, which can represent loading conditions of structural elements in any structure. The Multi-Directional Hybrid Testing System (MDHTS) at Polytechnique Montreal is an advanced structural testing system that can be used to study the response of large-scale structural components under such complex loading and boundary conditions. During the last three years, two experimental programs were conducted by researchers at Polytechnique Montreal and McGill University to study the seismic response of steel I-shaped columns for steel braced frames and moment-resisting frames using the MDHTS. The objectives

of these studies include: 1) generating physical test data on steel I-shaped columns, 2) verifying the column response as observed in numerical simulation, and 3) implementation of hybrid simulation. In this paper, the features and capabilities of the MDHTS are first described. Three examples of experimental testing of steel I-shaped columns, as part of concentrically braced frames (CBFs) and moment-resisting frames (MRFs), under multi-directional cyclic/seismic loading are presented.

## 2 MULTI-DIRECTIONAL HYBRID TESTING SYSTEM (MDHTS)

### 2.1 Physical capabilities

The MDHTS is an advanced structural testing system designed to impose any combination of forces and displacements to large-scale test specimens using a sophisticated control system. The system can be used to perform multi-axis static, quasi-static cyclic, pseudo-dynamic, and/or hybrid tests. The system is shown in Fig. 1 with an I-shaped steel column specimen installed. It includes a rectangular upper platen with 2.5 m x 3.5 m 0.625 m dimensions. The platen is a stiff multi-cellular steel construction that can be displaced along 6 degrees-of-freedom (DOFs) using a total of eight actuators: four 1.8 MN vertical actuators placed at the four corners and four 1.0 MN horizontal actuators (two in each horizontal direction). A lower platen with the same dimensions is anchored to the laboratory's strong floor. The specimens are placed between the two platens for testing. The four vertical actuators are connected to the upper platen and the lower platen/strong floor assembly and their length can be adjusted to achieve test heights varying from 4.0 m to 8.0 m. The four horizontal actuators are connected between the upper platen and the laboratory L-shaped reaction wall.

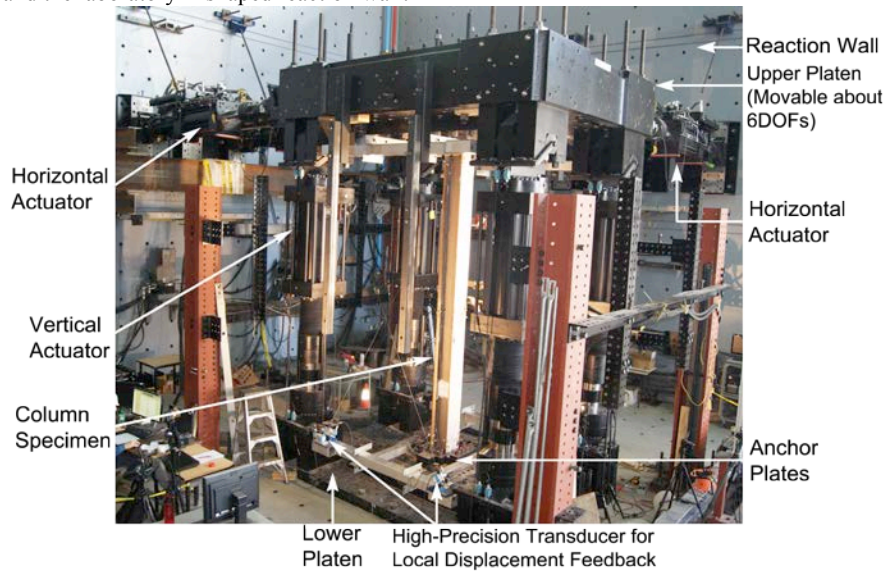


Figure 1. I-shaped column specimen in the Multi-Directional Hybrid Testing System at Polytechnique Montreal.

In the system, axial displacements and forces in each actuator are monitored and transformed into displacements or forces along three translational and three rotational DOFs at a control point located at the center of the bottom surface of the upper platen. This transformation is performed by a dedicated routine implemented in the MTS FlexTest 793 controller. Also, the controller is designed to function using net relative displacements measured between the top and bottom ends of the specimens, thus eliminating displacements induced by deformations in the platen and the connections of the specimens to the platen. This local control displacement feedback is obtained using eight high-precision digital transducers mounted on

rigid frames attached to the specimen ends (see Fig. 1). The control mode can be in either load- or displacement-controlled, or any combination of the two. Typically, the test specimens are rigidly connected to the platens at both ends, as discussed in the next section. Forces and displacements are then applied at a specimen top ends through the upper platen. For column testing under axial loads, the top end condition can be pinned (moments are set to zero), fixed (displacements are set to zero), or semi-rigid (by specifying the relationship between end moment and rotation in the control system).

The vertical and horizontal actuators are placed on a 2 m by 3 m horizontal grid. As shown in Fig. 1, the X and Y axes correspond to the horizontal directions parallel to the 2 m and 3 m dimensions, respectively. The Z axis represents the vertical direction. The translational and rotational capacities at the control point can be calculated based on the stroke capacity of each actuator (see Table 1). The total force and displacement capacities of the system in each DOF are given in Table 1. If needed, larger horizontal displacements towards one direction can be achieved by offsetting the upper platen in the opposite direction before installing the test specimen. The rotational capacity about the three axes of the MDHTS are presented in Table 1. The moment capacities were calculated assuming that the specimen is centered in the test setup and no axial load is applied. Moment capacities reduce in presence of axial loads but this effect can be mitigated by placing the specimen away from the center of the platen.

Table 1. Translational and rotational capacities of the MDHTS (at control point).

Translational Capacities			Rotational Capacities			
Plane Axis	Vertical Z	Horizontal X & Y	Plane Axis	Vertical About X	Vertical About Y	Horizontal About Z
Force (kN)	$\pm 7200$	$\pm 2000$	Moment (MN-m)	$\pm 10.8^1$	$\pm 7.2^1$	$\pm 5.0$
Displacement (mm)	$\pm 300$	$\pm 375$	Rotation (rad.)	$\pm 0.122$	$\pm 0.300$	$\pm 0.250^2$

<sup>1</sup>From vertical actuators only, with no concomitant axial load.

<sup>2</sup>With no concomitant translations.

## 2.2 Hybrid simulation capabilities

Hybrid simulation combines computer simulations with physical testing to offer a cost-effective option for evaluating the seismic performance of structures. In a hybrid simulation, the structure is divided into two parts. The first part consists of the elements of the structure whose responses are “well understood” and can be reliably predicted by using a finite element analysis software. This part represents the numerical substructure of the structure under investigation. The second part includes the elements expected to exhibit complex inelastic response and, possibly, strength deterioration or buckling. These element(s) form the experimentally substructure of the hybrid model. At every analysis step, displacements from the analysis are imposed on each test specimen and force feedback is used to determine the displacements in the subsequent step.

There are three main components in hybrid simulation: the computational driver, which houses the finite element (FE) model, the physical testing system that includes the FlexTest controller and experimental equipment, and the middleware that mediates the communications between the former two. The *OpenFresco* program [1] is used as the middleware because of its robust, flexible and easily extensible environment. It also supports a large variety of computational drivers such as the *OpenSees* program [2] used in the studies described in this article. The MDHTS includes two interfaces between *OpenFresco* and the FlexTest controller: 1) *MTS Computer Simulation Interface (CSI)* [3]; and 2) *Mathworks Simulink* platform with Scramnet communication [4]. The first interface is simpler because it handles command and feedback signals; however, there is no possibility to modify the signals during the analysis. The *Simulink* interface offers more flexibility to access and modify the command and feedback signals. Furthermore, *Simulink* includes several features and tools to customize the simulation procedure to suit user’s needs. For instance, filters and equations can be added or the predictor-corrector algorithm can be modified.

At the time of writing, hybrid simulation capabilities have been fully implemented and verified through preliminary column tests. The tests revealed that frictional forces developing in the actuator swivels (see Section 3.2) pose a challenging problem as they represent fictitious feedback forces that add

to the specimen force response. Different schemes are being examined to overcome this difficulty. One approach is to remove frictional forces measured during cyclic tests, which is achieved by simply subtracting the friction forces measured along each DOF in *Simulink*. Another technique is to add in parallel with the structure FE analysis an *OpenSees* model of the MDHTS setup in which negative frictional response is assigned to the actuator swivels. A second approach is to correct the feedback forces based on the anticipated stiffness of the specimen in each DOF. The correction is applied until friction is overcome in the actuator swivels and the measured forces reflect the specimen anticipated stiffness.

### 3 TEST PROGRAMS ON I-SHAPED STEEL COLUMNS

The first testing programs were performed on 4 m tall I-shaped steel columns used in concentrically braced frames (CBFs) and moment resisting frames (MRFs). These tests were conducted to validate the physical test setup and controller capabilities, verify the numerical models, and study the seismic response of steel columns in order to improve seismic design guidelines. These testing programs involved pre-determined displacement-loading protocols. The tests generated new data on the axial load (buckling) capacity, flexural strength and inelastic rotational capacities of steel columns subjected to various loading conditions expected under severe seismic loading. Three examples are presented herein to illustrate the capabilities of the testing system. Prior to performing the tests, preliminary finite element simulations were carried out to verify the adequacy of the connections of the test specimens to the platens and acquire insight on the specimen responses.

#### 3.1 Finite element analysis of the MDHTS

A three-dimensional finite element model of the MTDHS and the test specimens was created in the *Abaqus* software [5] with eight-node solid elements. The concrete strong floor of the laboratory was also included in the model. The actuators were not considered in this model; they were replaced by concentrated loads or displacements acting in the directions of their longitudinal axes. The column specimens were modelled using either elastic or inelastic material properties. For the latter, residual stresses, out-of-straightness imperfections and geometric nonlinearities were included in the analysis. In the FE model, special attention was devoted to the column end details used to develop fully rigid connections between the column specimens and the platens. The connection is shown in Fig. 2a. Columns were shipped to the laboratory with shop-welded 76 mm thick end plates. The plates were assembled to 140 mm thick, 1.95 m by 1.40 m large, transition steel plates using 51 mm diameter high-strength A574 socket head cap screws, pre-tensioned to 60% of ultimate ( $T_o = 1100$  kN). Thick (100 mm) plate washers were placed between the underside of the screw heads and the column end plates to achieve uniform compression between the end plates and transition plates. The number of screws was adjusted to prevent plate separation under the full flexural and axial tensile strength of the columns. The transition steel plates were also connected to the platens using pre-tensioned high-strength anchor rods. In the model, all plates, screws, rods, and washer plates were explicitly modelled, including pretension forces, contact and friction responses to assess stress levels in the components and column end fixity conditions. The system's ultimate capacity was designed for a W610x217 cross-section as discussed in Elkady [6].

Examples of nonlinear FE analyses are illustrated in Fig. 2 for the W250x101 shape representative of a CBF column. In Fig. 2b, the stress distribution in the end connection is examined when the specimen is subjected to 12% story drift inducing strong-axis bending. Von Mises stresses did not exceed the yielding stress in any of the bolts, transition plates, or platens. From the analysis, the elastic lateral stiffness of the column assembly is 4.95 kN/mm, close to the 5.25 kN/mm value obtained from theory. In Fig. 2c, elastic flexural buckling about weak-axis is studied for fixed end conditions. In the analysis, elastic material properties were used and a downward vertical displacement was gradually imposed to the upper platen at the vertical actuator locations until buckling occurred. From the computed elastic buckling load, a  $K$  factor of 0.53 was estimated for the column, close to the 0.50 value for ideal fixed-fixed end conditions.

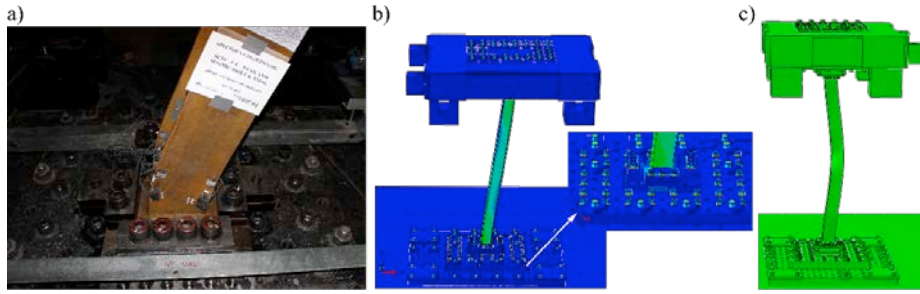


Figure 2. a) Column base plate detail (photo taken after development of plastic hinge in the column); b) Von Mises stress in the base plate detail under 12% story drift in strong-axis of the column; and c) buckled column in the MDHTS under vertical displacement.

### 3.2 Cyclic testing of steel I-shaped CBF column

The buckling response of a 4 m tall W250x101 column specimen was examined. The specimen was subjected to an axial compression load equal to 4112 kN corresponding to 90% of the column compressive yield strength ( $P_y$ ) which was applied in the load-controlled mode and maintained throughout the test. A lateral displacement of 100 mm ( $= 2.5\% h$ ) was then applied at the column top end, followed by the rotation history shown in Fig. 3a. Both the applied story drift and end rotations induced flexure about the column weak-axis and were applied using displacement-controlled mode. The specimen was rigidly connected at its bottom end. These loading and boundary conditions reflected those expected for first-storey columns in steel CBFs subjected to seismic loading. The measured yield strengths were 402 MPa and 398 MPa for the web and flanges of the specimen's cross-section, respectively.

Column axial shortening and weak-axis bending moment at the column top end are plotted against the applied top end rotation in Figs. 3b and c. For such a test under constant axial load, axial shortening is a good indicator of column flexural buckling. As illustrated, the first positive end rotation excursion that was applied reduced the top end moment and did not have adverse effect on the column. Plastic hinging formed when applying the subsequent negative end rotation, which resulted in column axial shortening. In subsequent end rotation cycles, more pronounced shortening took place when imposing negative end rotations. Column flexural buckling initiated when applying top negative rotation of -0.04 rad (point E in Fig. 3) and the column lost its axial load carrying capacity at a rotation of -0.038 rad in the same half-cycle. Fig. 3d shows the column buckled shape at the end of the test.

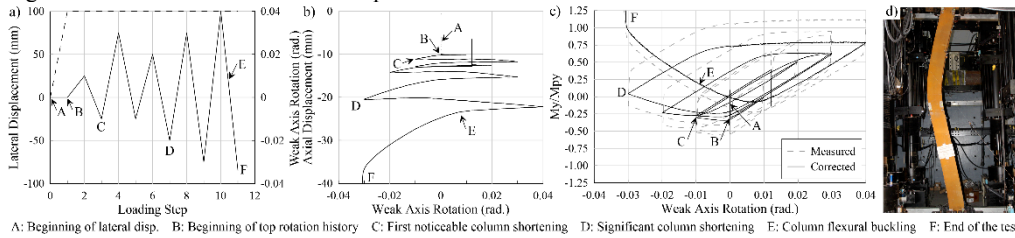


Figure 3. a) Applied displacement protocol; b) Column axial shortening vs rotation at the top end; c) Normalized weak-axis moment vs rotation at the top end; and d) Buckled shape at the end of the test.

In Fig. 3c, the sharp variations in top end moments at every end rotation reversal reveal frictional resistance developing in the swivels of the actuators. Although it cannot be monitored in the test setup, this frictional resistance is mainly attributed to the vertical actuators because of their larger size and the tension load they carried to apply the column axial load. For this specimen, that rotational resistance approximately represented 0.5 times the section plastic moment  $M_{py}$ , which is significant. However, since the axial load was

constant, the friction in every half-cycle was assumed to be constant and equal to the value observed at the beginning of the cycle and could then be easily removed to obtain the actual column flexural strength.

### 3.3 Seismic testing of steel I-shaped CBF column

Another test was performed on a 4 m tall W250x101 specimen to study the response of the 8<sup>th</sup> story column as part of a 10-story tension-only X-bracing system. The material properties and end conditions for this specimen were the same as described in Section 3.2. The objective of this test was to evaluate the acceptance criteria specified for columns in the ASCE 41-13 standard [7]. The loading protocol applied in this test is shown in Fig. 4a. It was extracted from the nonlinear response history analysis of the steel braced frame using the *OpenSees* finite element structural analysis platform. The gravity load was first imposed to the specimen. This was followed by the histories of axial force, story drift and relative end rotation about strong axis resulting from two consecutive applications of the same ground motion. The scale factor of the second ground motion was two times of the scale factor of the first one. Lastly, a constant axial load equal to 0.9 of nominal compressive strength of the column  $P_n$  was applied together with stepwise increasing cyclic rotations at the column top end until column buckling. Axial forces were applied in load-controlled mode, whereas displacement-controlled mode was used to impose lateral displacements and end rotations.

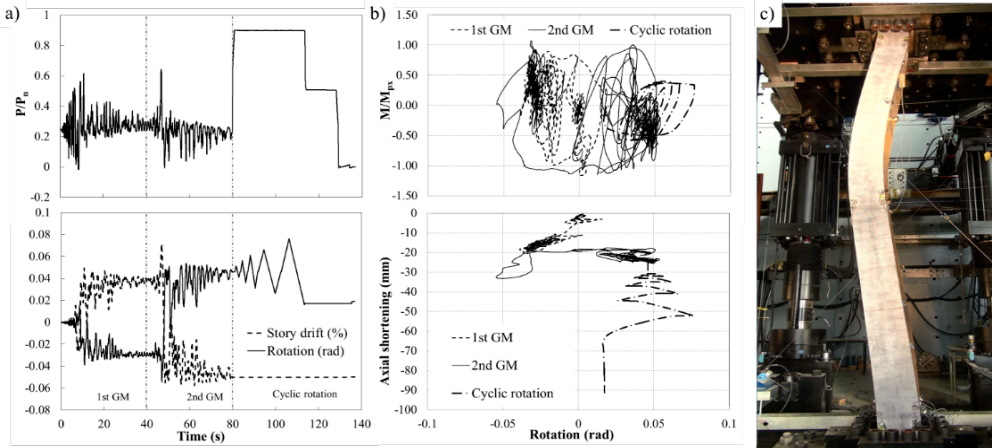


Figure 4. a) Applied axial load, story drift and top end rotation, b) Top end moment about strong axis and axial shortening vs top end rotation; and c) Buckled shape at the end of the test.

The measured top end, strong axis moment and column axial shortening are presented in Fig. 4b as a function of strong axis to end rotation. The column could withstand the two ground motion sequences without buckling and flexural strength degradation. During the first ground motion, the specimen experienced a total shortening of 20 mm. At the beginning of the second sequence, axial shortening continued but it was interrupted due to a large inelastic story drift and end rotation excursion that occurred in the opposite direction. The column could then maintain its axial and flexural resistances up to the end of the second ground motion. During the two ground motion histories, frictional resistance by the test setup was not significant because axial loads were relatively low and the column was bent about strong axis and offered much larger lateral resistance.

In the last part of the test, cyclic end rotation was applied in combination with high constant axial load and the specimen exhibited a reduced flexural strength and experienced additional axial shortening. The column eventually failed by weak axis flexural buckling with some torsional response, as shown in Fig. 4c. According to ASCE 41, this column was not capable of sustaining any inelastic rotation demands. The experiment clearly showed that the column could in fact achieve considerable rotational ductility, even when carrying a large compressive axial load.



### 3.4 Cyclic testing of deep I-shaped MRF columns with flexible boundary conditions

The third testing program investigated the cyclic behaviour of typical first-storey interior deep columns as part of steel MRFs designed in highly seismic regions. Till recently, experimental data on deep steel columns (depth > 400mm) was limited due to equipment limitations and complexity of testing such deep members. To this end, ten 4 m long I-shaped specimens were tested. Six specimens utilized a W610x217 cross-section. W610x125 cross-section was used for the rest. The column specimens were subjected to a constant compressive axial load combined with cyclic lateral drifts. In the strong-axis direction, two specimens had fixed boundary conditions at both ends while eight specimens had a fixed base and a flexible top end. The latter boundary conditions capture the flexibility of the beam-to-column connection at the top of a steel column in a MRF. Such realistic boundary conditions had never been investigated in past experimental studies. To simulate flexible boundary conditions, a pre-described rotation about the X axis was applied at the column top end. This rotation was synchronized with the imposed lateral drift history. This rotation was obtained from detailed FE analysis conducted prior to the actual test as discussed in Elkady and Lignos [8]. This rotation is set to enforce the moment inflection point to be at a distance equal to  $0.75 L$  measured from the column base, during the elastic range of the lateral protocol.

To demonstrate the effect of the flexible boundary conditions, specimen C1 and C3 are compared in Fig. 5. Specimen C1 utilized fixed boundary conditions at both ends while specimen C3 had a fixed base and flexible top end. Both specimens utilized a W610x217 cross-section and were subjected to an axial load level equal to  $20\% P_y$  combined with a unidirectional symmetric cyclic lateral loading protocol about their strong-axis. The end moment, normalized by plastic flexural strength  $M_{px}$ , versus chord-rotation relation at both column ends is shown in Fig. 5. The global deformation profile at a chord-rotation equal to 4% radians is also shown in the same figure.

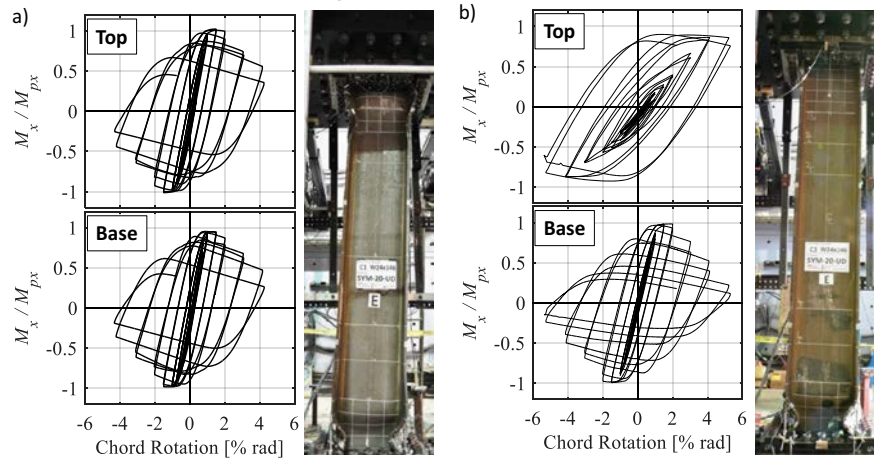


Figure 5. Normalised moment-rotation relation at both column ends and the global deformation profile at 4% rad for: a) specimen C1; (b) specimen C3.

Fig. 5a shows that the moment-rotation relation at both ends of specimen C1 are more-or-less the same. This attributed to the similar boundary conditions at both ends that lead to the simultaneous occurrence of yielding and local buckling. This however is not representative of first-story MRF columns where plastic hinging is expected to occur only at the base. Based on Fig. 5b, the base of specimen C3 behaved similarly to that of specimen C1. However, local buckling occurred earlier in specimen C1 due to its larger lateral flexural stiffness compared to specimen C3. Furthermore, specimen C1 deteriorated slightly faster in flexural strength compared to specimen C3, particularly at chord-rotations larger than 3% rad. Most importantly, local buckling did not occur at the top end of specimen C3 except at 4% rad. At this level of drift, the column base had deteriorated significantly and force redistributions lead to an increased demand on the

column top. This can be observed from the global deformation profile in Fig. 5b where local buckling is only evident at the base. Finally, specimen C1 experienced an axial shortening level of about 4%  $L$  at 4% rad. This is almost double the axial shortening experienced by specimen C3 at the same rotation.

#### 4 CONCLUSIONS

In this paper, the Multi-Directional Hybrid Testing System (MDHTS) at Polytechnique Montreal was introduced and its main features and capabilities were described. The results of finite element analysis of the system under critical loading scenarios were presented to verify the influence of the anchor plates and the test setup on the stiffness and strength of specimens. The results of full-scale tests of steel I-shaped columns part of CBFs and MRFs were presented. It was shown that the testing system is capable of applying different loading protocols at any DOF at the top end of the specimens in either load- or displacement-controlled mode or combination of these modes. The movable upper platen of the testing machine can also reproduce nearly fixed or flexible end conditions. It was also shown that the MDHTS can be used to generate reliable data on inelastic response of steel columns including plastic hinging as well as local and global buckling under seismic induced cyclic demands. Future research projects are being planned to study other structural components part of steel and reinforced concrete structures under various loading conditions. Hybrid simulations will also be performed on steel braced frames, moment frames and concrete shear walls using the MDHTS.

#### ACKNOWLEDGEMENTS

Funding for the test equipment described in this article was obtained from the Canadian Foundation for Innovation of the Government of Canada and the Government of Quebec. In-kind contributions from industrial partners MTS Systems Corporation, Minneapolis, Minnesota, LCL Bridge Inc., Montreal, Quebec, and Industries Desormeaux, Montreal Quebec. Funding for the projects described in this article was provided by the Natural Sciences and Engineering Council (NSERC) of Canada, the Canadian Institute of Steel Construction (CISC) (formerly Steel Structures Education Foundation) and the CEISCE Strategic Network of the Fonds de recherche en Nature et Technologies (FRQNT) of the Quebec Government. The ADF Corporation Inc. donated the material and fabrication for four specimens of the third experimental program.

#### REFERENCES

- [1] OpenFresco, “*Open Framework for Experimental Setup and Control*”, 2012, <http://openfresco.neesforge.nees.org>.
- [2] McKenna, F. and Fenves, G.L. “*Open System for Earthquake Engineering Simulation (OpenSees)*”, Pacific Earthquake Engineering Research Center (PEER), University of California, Berkeley, CA, 2004, <http://opensees.berkeley.edu/index.html>.
- [3] MTS, “*Civil engineering testing solution*”, 2015, <http://www.mts.com>.
- [4] MathWorks, “*MATLAB: The Language of Technical Computing*”, MathWorks Inc., Natick, MA, 2012.
- [5] Simulia. “*Abaqus FEA*, 2011”, [www.simulia.com](http://www.simulia.com).
- [6] Elkady, A. “*Collapse Risk Assessment of Steel Moment Resisting Frames with Deep Wide-Flange Columns in Seismic Regions*”, PhD Dissertation, McGill University, Department of Civil Engineering and Applied Mechanics, 2016.
- [7] ASCE, “*Seismic evaluation and rehabilitation of existing buildings*”, ASCE/SEI 41-13, American Society of Civil Engineers, Reston, VA, 2013.
- [8] Elkady, A. and Lignos, D.G. “Dynamic Stability of Deep and Slender Wide-Flange Steel Columns – Full Scale Experiments”, *Proceedings of the Annual Stability Conference, Structural Stability Research Council*, Orlando, Florida, 2016.